doi number

J. Braz. Chem. Soc., Vol. 00, No. 00, 1-10, 2015.
Printed in Brazil - ©2015 Sociedade Brasileira de Química
0103 - 5053 $6.00+0.00

Article

TiO_2 Supported on HZSM-11 Zeolite as Efficient Catalyst for the Photodegradation of Chlorobenzoic Acids

Juan P. Montañez,[a,b] Silvina Gómez,[b,c] Ana N. Santiago[a,b] and Liliana B. Pierella*[*,b,c]

[a]*Instituto de Investigaciones en Físico-Química de Córdoba (INFIQC), Departamento de Química Orgánica, Facultad de Ciencias Químicas, Universidad Nacional de Córdoba, Córdoba, 5000, Argentina*

[b]*Consejo Nacional de Investigaciones Científicas y Técnicas (CONICET), C1033AAJ, Argentina*

[c]*Centro de Investigación y Tecnología Química (CITeQ), Facultad Córdoba, Universidad Tecnológica Nacional, Córdoba, 5000, Argentina*

The photocatalytic decomposition of 2-, 3- and 4-chlorobenzoic acids (2CB, 3CB and 4CB, respectively) with TiO_2 loaded on HZSM-11 zeolite was investigated. The optimum decomposition rate of 2CB was obtained with TiO_2/HZSM-11(30%) (TiO_2 30 wt.%) catalyst at a concentration of 1 mg mL^{-1}. 2CB and 3CB decompose at similar rates, but 4CB remains adsorbed on TiO_2/HZSM-11(30%) without further degradation. This absorption is attributed to the relative positions of Cl and COOH groups on 4CB. However, this compound can be partially degraded and/or removed from aqueous solutions by TiO_2/HZSM-11(50%) catalyst or HZSM-11 zeolite. TiO_2/HZSM-11(30%) is stable; it retains its photocatalytic properties after nine cycles, can be easily removed and immediately reused. These are important advantages of TiO_2/HZSM-11(30%) over unsupported TiO_2, making it a good photocatalyst for the treatment of polluted water. On the other hand, HZSM-11 could be used to selectively adsorb 4CB, thus becoming an alternative method of environmental remediation.

Keywords: aromatic acids, heterogeneous photocatalysis, supported catalysts, TiO_2, zeolite

Introduction

Aromatic acids are used in wood preservatives, paints, vegetal fibers and leather due to their bactericidal activity.[1] They are also used as raw materials for the synthesis of herbicides, pesticides, pharmaceuticals and dyes.[2-4] Furthermore, they are end products of the biodegradation of aromatic industrial contaminants.[2] Chlorobenzoic acids are environmental pollutants produced mainly by the biodegradation of polychlorinated biphenyls and some herbicides.[5] One of them, 2-chlorobenzoic acid (2CB) is present in effluents from the pharmaceutical industry, and as such, it can contaminate natural water courses.[6] These chloroaromatic acids are persistent in the environment, adversely affecting the flora and fauna.

Many different methods have been used to remove these contaminants from wastewater, photodegradation by UV radiation being one of the most effective. Through this process a large variety of organic products can be completely mineralized.[6] TiO_2 is the most widely photocatalyst used; however, once the reaction has been completed this compound cannot be easily removed from an aqueous medium as it remains in suspension and expensive special filtration equipment has to be used. An alternative is the use of TiO_2 immobilized on a porous material such as zeolites; these materials have channels, pores and cavities which may improve the selectivity of TiO_2 and increase the reactivity of the substrate to be oxidized, leading to an increase of its photocatalytic activity.[7] Zeolites have proven to be efficient support materials for titania in the photodegradation of salicylic acid (TiO_2/MCM-41),[8] an azo-dye (TiO_2/β and TiO_2/montmorillonite),[9] ethinyl estradiol (TiO_2/low-silica X zeolite),[10] EDTA (TiO_2/ZSM-5)[11] and amoxicillin (TiO_2/natural zeolite).[12]

In particular, ZSM-11 zeolite framework structure is very similar to that of ZSM-5 zeolite.[13] Unlike this zeolite structure, ZSM-11 zeolite possesses straight intersecting channels having same elliptical pore size (5.3 × 5.4 Å).

*e-mail: lpierella@scdt.frc.utn.edu.ar

This property enhances the molecular diffusion, inside the zeolite cavities, by reducing the tortuosity factor. Also, ZSM-11 zeolite does not lose their initial crystalline structure after chemical and thermal treatments, unlike other zeolites, e.g., Y zeolites.[14]

In a previous report[15] this catalyst has proven to be effective to degrade dichlorvos, a non-ionizable insecticide, under UV-irradiation. In this study, the photocatalytic activity of TiO_2 supported on HZSM-11 zeolite was evaluated in 2CB degradation, considering the effects of catalyst concentration, wt.% of TiO_2 loaded on HZSM-11, and the repeatability of the photocatalytic activity of the catalyst after multiple cycles of reuse. The degradation rate of three ionizable compounds, 2CB and its isomers 3- and 4-chlorobenzoic acids (3CB and 4CB, respectively), were also compared under conditions similar to solar radiation.

The main goal of this research is to expand the number of compounds that can be degraded by this catalyst, because it is highly desirable that a catalyst can degrade different pollutants. This property is very useful to develop an adequate and efficient methodology for effluent and natural watercourses remediation. To our knowledge, studies on the photodegradation of these three isomers (2CB, 3CB and 4CB) by TiO_2 supported on HZSM-11 zeolites have not yet been reported.

Experimental

Reagents

HZSM-11 zeolite was prepared using the following reactants: sodium aluminate ($NaAlO_2$, Johnson Matthey Electronics), tetrabutylammonium hydroxide (TBAOH, Fluka), silicic anhydride (Fluka) and distilled water. Titanium(IV) isopropoxide, 2CB, 3CB and 4CB acids were purchased from Aldrich and used as received. Ethanol (Cicarelli) was employed. P25, standard TiO_2, was kindly supplied by Degussa.

Preparation of TiO_2/HZSM-11-supported catalyst

The parent Na-ZSM-11 zeolite (Si/Al = 17) was obtained by known hydrothermal crystallization methods.[15] The ammonium form of the zeolite (NH_4-zeolite) was prepared by ion exchange from Na-zeolite with 1 mol L^{-1} ammonium chloride solution at 80 ºC for 40 h. Finally, NH_4-zeolite was dried at 110 ºC, treated in a nitrogen flow at 500 ºC during 8 h and then calcined in air at the same temperature for 10 h, obtaining the HZSM-11 zeolite.

The supported catalysts were prepared by mixing appropriate amounts of titanium(IV) isopropoxide and zeolite in ethanol. This mixture was mechanically stirred for 4 h at ambient temperature, and then the solvent was removed by evaporation. The mixture was then dried at 110 ºC and calcined in air at 450 °C. The amount of titanium(IV) isopropoxide was changed with the purpose of generating *in situ* theoretical TiO_2 concentrations of 3, 10, 30 and 50 wt.% in the final solid. They were labeled TiO_2/HZSM-11(3%), TiO_2/HZSM-11(10%), TiO_2/HZSM-11(30%) and TiO_2/HZSM-11(50%), respectively. Commercial TiO_2 (P25, Degussa) was also employed for comparison.

Characterization

The catalysts were previously characterized by X-ray diffraction (XRD), transmittance Fourier transform infrared spectroscopy (FTIR), specific surface areas by the Brunauer-Emmett-Teller (BET) method, scanning electron microscopy (SEM), inductively coupled plasma optical emission spectroscopy (ICP-OES), and UV-Vis diffuse reflectance spectroscopy (DRS).[15]

Photocatalytic activity evaluation

All experiments were performed in triplicate in a borosilicate water-jacketed glass reactor, irradiated with two Philips Master HPI-T Plus 400 W lamps water-air cooled (Figure 1), with an emission interval ranging from 350 to 650 nm, according to the manufacturer's specifications. The emission spectrum of these lamps is very similar to sunlight emission spectrum at sea level.

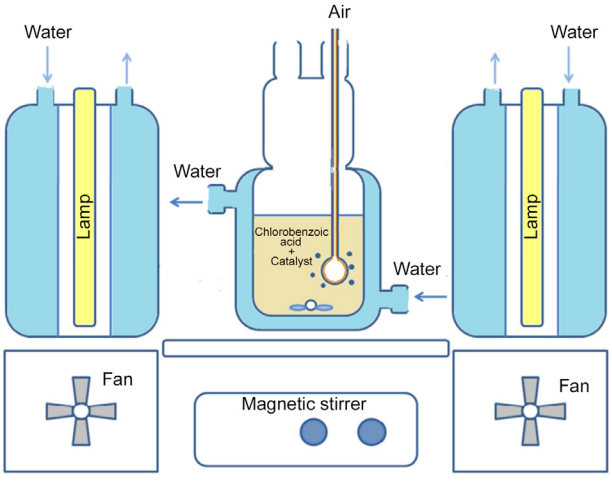

Figure 1. Experimental photocatalytic reactor.

Photocatalytic activity measurements were conducted on the catalysts TiO_2/HZSM-11(3%), TiO_2/HZSM-11(10%), TiO_2/HZSM-11(30%), and TiO_2/HZSM-11(50%) in different concentrations: 0.25, 0.5, 1 and 2 mg mL^{-1}. For

this purpose, a 10^{-4} mol L^{-1} aqueous solution of 2CB, 3CB or 4CB containing the photocatalyst in suspension was allowed to equilibrate in the dark for 30 min with mechanical stirring and without air bubbling. Subsequently, this mixture was irradiated for 4 h and atmospheric air bubbling. Aliquots were withdrawn at specific time intervals and analyzed after filtration with 0.45 μm Millipore membrane to remove catalyst particles. The starting aliquot corresponds to the time at which the lamps were turned on.

The aliquots were then analyzed on a Waters 1525 high-performance liquid chromatography (HPLC) equipment with an Agilent Zorbax Eclipse XDB-C18 5 μm column and a UV-Vis photodiode array detector operating between 190-370 nm.[1] A mixture of methyl alcohol (40% v/v) and acetic acid/sodium acetate buffer (pH 4, 60% v/v) was used as mobile phase at a flow rate of 0.3 mL min^{-1}. Twenty-five milliliters of each aliquot were injected and analyzed at a wavelength of 236 nm.[6] Direct photolysis of 2CB was also studied irradiating a 2CB solution for 4 h in the absence of the photocatalyst.

Photodegradation reactions with catalysts TiO_2/HZSM-11(3%), TiO_2/HZSM-11(10%), TiO_2/HZSM-11(30%) and TiO_2/HZSM-11(50%) were compared with the uncharged matrix (HZSM-11) and unsupported TiO_2.

In addition, adsorption studies of 2CB or 4CB were carried out at room temperature (25 ºC). For this purpose, a 10^{-4} mol L^{-1} aqueous solution of 2CB or 4CB containing the photocatalyst in suspension was keep in the dark for 24 h with mechanical stirring and air bubbling. Aliquots were withdrawn at specific time intervals and analyzed as described above.

The conservation of the photocatalyst activity was determined by the percentage of degradation of 2CB after irradiation, and was calculated as follows for every cycle:

$$\text{Degradation percentage} = (1 - C / C_0) \times 100 \quad (1)$$

where C is the 2CB concentration in the solution after 2 h of irradiation, and C_0 is the initial concentration (10^{-4} mol L^{-1}).

Results and Discussion

Characterization of TiO_2/H-zeolite catalysts

XRD analysis

In order to confirm the structure and crystallinity of TiO_2/zeolite catalysts, an XRD study was carried out. Figure 2 shows the XRD patterns of HZSM-11 (a) and different titania-supported catalysts (b-e). For comparative purposes, the diffraction pattern of commercial P25 titania (f) is also included. Figure 2 shows the characteristic signal of the parent HZSM-11 catalyst at 2θ angles of 23-24º and 7-9º, which were assigned to (332), (303) and (101), (200) planes, respectively.[16] The XRD pattern of TiO_2/H-ZSM-11(3%) catalyst (Figure 2b) was essentially the same as that of the original HZSM-11 (Figure 2a). TiO_2/HZSM-11 prepared in this study showed diffraction peaks at 25.4, 48.2, 54.9 and 55.4°, which were assigned to the characteristic reflections from (101), (200), (211) and (106) planes of anatase, respectively.[17] In the diffraction pattern of TiO_2/HZSM-11(10%), the peak at (101) is barely observed, but the other three peaks are not clearly observed since the amount of TiO_2 would not be enough to give clear diffraction peaks.

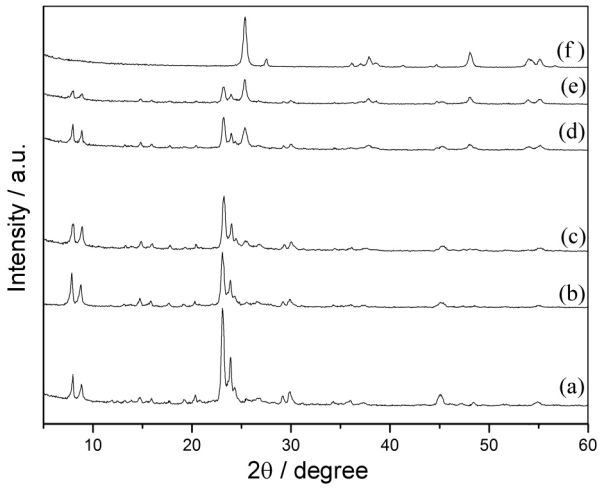

Figure 2. XRD pattern of (a) zeolite HZSM-11, (b) TiO_2/HZSM-11(3%), (c) TiO_2/HZSM-11(10%), (d) TiO_2/HZSM-11(30%), (e) TiO_2/HZSM-11(50%) and (f) P25 Degussa.

The peak intensity at 2θ = 25.4° increased with an increasing amount of TiO_2 loaded on HZSM-11. A similar XRD pattern was obtained for TiO_2/zeolites (Y, A and BEA), as reported previously.[18,19] Simultaneously with the increase in the TiO_2 load, a small decrease in the intensity of HZSM-11 diffraction peaks was observed. However, this decrease can be attributed to a dilution effect of the zeolite matrix in the catalyst.

On the other hand, no peak assigned to rutile phase (2θ = 27.4º) was observed in the XRD patterns of all TiO_2/HZSM-11 catalysts used in the present study.

FTIR spectra

Figure 3 shows the FTIR spectra of bulk TiO_2, bulk zeolite and TiO_2/HZSM-11(wt.%) in the range of 1800-400 cm^{-1}. All the zeolitic materials present vibrations assigned to the internal bonds of a TO_4 tetrahedral structure (T = Si or Al) that are insensitive to changes in the zeolite

structure, 1250-950, 850-700 cm^{-1} and the signals at 500 to 420 cm^{-1} being attributed to asymmetrical stretching, to the symmetrical stretching and to (O–T–O) deformation, respectively. Furthermore, vibrations assigned to the external bonds of the TO_4 tetrahedral structure, which are sensitive to changes in the structure, can also be observed. These vibrations, in the region between 650 and 500 cm^{-1}, are attributed to those of double rings consisting of five atoms. A shoulder between 1050 and 950 cm^{-1} is assigned to the asymmetrical stretching of T–O–T bonds.[20]

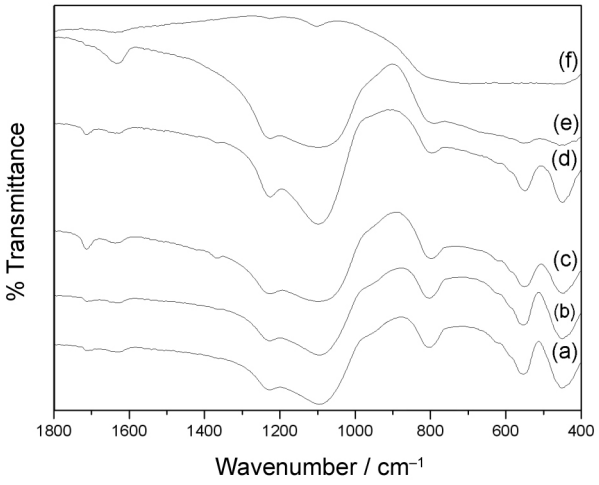

Figure 3. FTIR of (a) zeolite HZSM-11, (b) TiO_2/HZSM-11(3%), (c) TiO_2/HZSM-11(10%), (d) TiO_2/HZSM-11(30%), (e) TiO_2/HZSM-11(50%) and (f) P25 Degussa.

No band in the region near 960 cm^{-1} was detected, which could be assigned to the antisymmetric stretching vibration of the Ti–O–Si bonds.[19-21] Therefore, the replacement of the tetrahedral Si sites with Ti during preparation did not take place. So, we can conclude that TiO_2 was deposited on the surface of the zeolites.

TiO_2 crystallite size values, surface area (S_{BET}) and Ti, Si and Al content of the supported catalysts

The estimated TiO_2 crystallite size values (d), the surface area (S_{BET}) of the supported catalysts and Ti, Si and Al content (wt.%) are shown in Table 1.

The average crystallite size of TiO_2 on the zeolite matrix was estimated using XRD data and the Scherrer equation. The crystal size varies from 12 to 23 nm, rising with the increasing load of TiO_2, probably due to the aggregation of the TiO_2 particles on the surface of the zeolite.

The surface area (S_{BET}) of the synthesized materials was determined from the N_2 adsorption-desorption isotherms using the Brunauer-Emmett-Teller method. The adsorption-desorption isotherms of TiO_2/HZSM-11 samples exhibit characteristics similar to those of HZSM-11. According to IUPAC classification, they are type I isotherms, characteristic of microporous solids having relatively small external surfaces.[22] Also, the surface area of TiO_2/HZSM-11(3%) has similar characteristics to TiO_2/HZSM-11(10%). With an increase in TiO_2 loading, a linear decrease in the surface area of the samples can be observed. It could be possibly due to the deposit of TiO_2 particles on the HZSM-11 surface, thus, blocking the pores.

Table 1. Crystallite size of TiO_2, surface area, Ti, Si and Al content (wt.%) of TiO_2/HZSM-11 catalysts

Sample[a]	d / nm	S_{BET} / (m^2 g^{-1})	Ti	Si	Al
1	–	382	–	28.934	1.700
2	–	370	1.243	27.560	1.650
3	12.04	365	4.846	25.609	1.502
4	18.86	309	16.756	22.812	1.342
5	22.98	255	27.200	21.450	1.245

[a]1: HZSM-11, 2: TiO_2/HZSM-11(3%), 3: TiO_2/HZSM-11(10%), 4: TiO_2/HZSM-11(30%) and 5: TiO_2/HZSM-11(50%).

Ti, Si and Al content of TiO_2/HZSM-11 catalysts were determined by ICP-OES. The Ti wt.% increased when TiO_2 loading increased, which is in good agreement with theoretical values.

UV-Vis DRS

The UV-Vis diffused reflectance spectra of zeolite matrix and TiO_2/HZSM-11 samples are shown in Figure 4. The diffuse reflectance spectrum of HZSM-11 (Figure 4a) consists of a single band at 210 nm arising from the Al–O charge-transfer transition of four-coordinated framework aluminum, characteristic of as-synthesized zeolites.[23] In the supported catalyst (Figures 4b-d), the absorption band at 200-250 nm is due to electron transfer from the ligand-

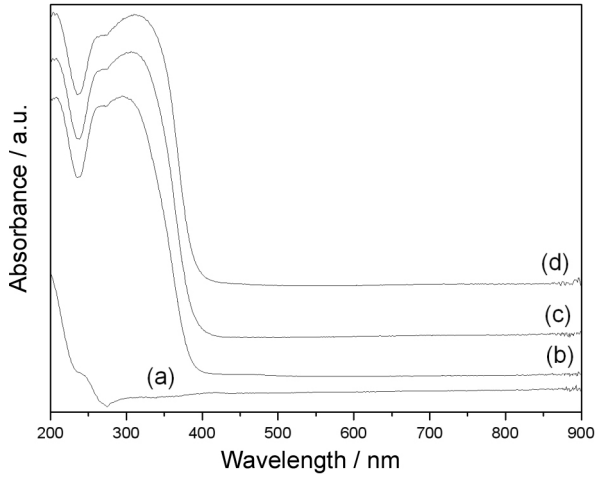

Figure 4. DRS of (a) zeolite HZSM-11, (b) TiO_2/HZSM-11(10%), (c) TiO_2/HZSM-11(30%) and (d) TiO_2/HZSM-11(50%).

oxygen to an unoccupied orbital of the Ti^{4+} framework.[24] The spectra are also characterized by an intense band centered at 320 nm, corresponding to charge transfer from the valence band (O 2p) to the conduction band (Ti 3d).[25]

The determination of the band gap (Eg) from the UV-Vis spectra is an alternative method to study the modification of the electronic properties of the TiO_2 species.[26] The band gap of TiO_2 can be affected by the particle size (quantum size effects) and the particle size could be affected by the thermal treatment temperature and of TiO_2 contents among others for TiO_2 hybrid systems.[27-29] The band gap energies were estimated from UV-Vis DRS spectra using the Kubelka-Munk remission function,[30] and the values (in eV) obtained were 3.25 (TiO_2/HZSM-11(10%)), 3.15 (TiO_2/HZSM-11(30%)) and 3.12 (TiO_2/HZSM-11(50%)).

The UV-Vis DRS spectra of the TiO_2/HZSM-11 samples showed the absorption threshold onset was scarcely shifted to the visible region when the TiO_2 concentration increased. As result, the Eg values present a small variation when varying TiO_2 content in the samples.

Effect of wt.% of TiO_2 loaded on HZSM-11

Figure 5 shows the photocatalytic decomposition of 2CB on TiO_2/HZSM-11(3%), TiO_2/HZSM-11(10%), TiO_2/HZSM-11(30%), and TiO_2/HZSM-11(50%) catalysts (1 mg mL^{-1} in all reactions). It also shows that 2CB does not photolyse and does not decompose with HZSM-11 zeolite.

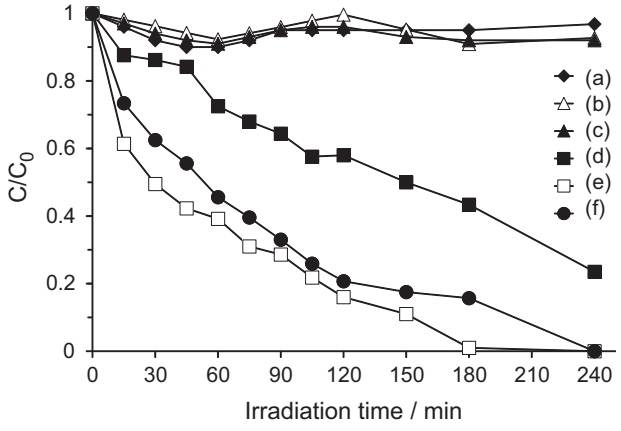

Figure 5. Photolysis (a) and photocatalytic decomposition of 2CB over (b) HZSM-11, (c) TiO_2/HZSM-11(3%), (d) TiO_2/HZSM-11(10%), (e) TiO_2/HZSM-11(30%) and (f) TiO_2/HZSM-11(50%) catalysts.

The degradation rate of 2CB increases with TiO_2 loading, except for the TiO_2/HZSM-11(50%) catalyst. In this case, its lower photocatalytic activity may be due to the agglomeration of TiO_2 particles, as observed by Ding *et al.*[31] on the degradation of phenol with TiO_2/silica gel catalysts.

TiO_2/HZSM-11(30%) was the most efficient catalyst, since 2CB was completely degraded after 3 h irradiation; it was, therefore, chosen for the following experiments.

2-Chlorophenol (2CP) is the major metabolite in the photodegradation of 2CB.[6,32] However, it was not observed in the reactions described in this work, although we tried to find this product using an aqueous solution of pure 2CP as standard. Probably 2CP forms slowly and it is immediately degraded by the photocatalyst in the reaction media.

Effect of catalyst concentration

A series of experiments was carried out to find the optimum amount of catalyst by varying TiO_2/HZSM-11(30%) concentration from 0.25 to 2 mg mL^{-1} (Figure 6). The decomposition rate increases with the amount of TiO_2/HZSM-11(30%) up to 1 mg mL^{-1}, but above this concentration the decomposition rate is not further increased.

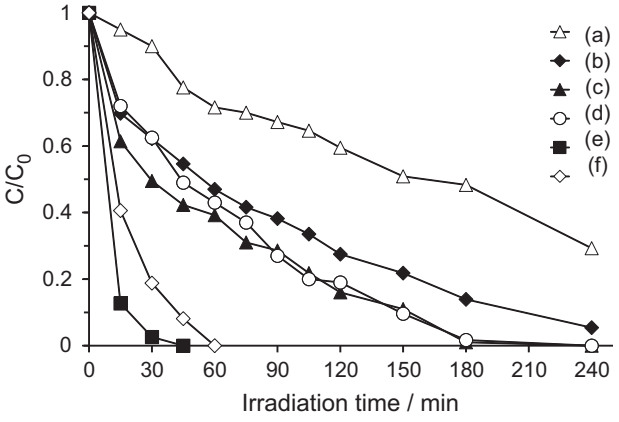

Figure 6. Effect of the amount of TiO_2/HZSM-11(30%) catalyst on the photocatalytic decomposition of 2CB: (a) 0.25 mg mL^{-1}, (b) 0.5 mg mL^{-1}, (c) 1 mg mL^{-1} and (d) 2 mg mL^{-1}. Unsupported TiO_2 (from Degussa) is also shown at (e) 1 mg mL^{-1} and (f) 0.3 mg mL^{-1}.

The concentration of the photocatalyst increases the amount of active sites as well, resulting in an improvement of the photocatalysis rate. However, when 2 mg mL^{-1} was added this rate was kept unchanged, probably due to the scattering of a fraction of incident radiation by the higher amount of particles present in the 2CB solution. This effect was previously observed by other authors.[7,33] Starting from a certain concentration of TiO_2/HZSM-11(30%) the 2CB solution becomes opaque due to suspended particles, preventing irradiation of active sites.[34]

The optimum amount of TiO_2 catalyst can reach values from 0.07 to 12 g L^{-1} depending on light intensity, wavelength, oxidizing agents, kind of contaminant, and so on.[33] In our work, the optimum amount of TiO_2/HZSM-11(30%) catalyst is 1 mg mL^{-1}, which corresponds to 0.3 g L^{-1} of TiO_2.

As seen in Figure 6, photocatalysis was faster when unsupported TiO_2 was used at a concentration of 1 or 0.3 mg mL^{-1}. The latter is equivalent to the TiO_2 load present in TiO_2/HZSM-11(30%), a concentration of 1 mg mL^{-1}. This may also be due to the total amount of particles present in the solution. Zeolite HZSM-11 allows the passage of radiation but it possibly scatters a fraction of the incident radiation, an effect that does not occur in solutions with unsupported TiO_2. However, although unsupported TiO_2 is a better photocatalyst in these reactions, it cannot be recovered easily[35] requiring expensive and laborious methods of separation of treated solutions. By contrast, the TiO_2/HZSM-11(30%) catalyst can be easily recovered from the reaction medium by filtration. Also, the spontaneous agglomeration of unsupported TiO_2 particles, when dispersed in aqueous media, may cause a rapid decrease in specific surface area, thereby photocatalytic activity decays.[36]

Considering that the solution of 2CB (pKa 2.92) has a pH of 4.1, the carboxylate anion:protonated acid ratio is 17:1. Since the point of zero charge of TiO_2 is ca. 6.25,[7] this catalyst surface is positively charged at this pH, and thus photocatalysis of this organic pollutant is promoted by the electrostatic attraction between TiO_2 and the anion of 2CB.

Leaching study of the catalyst

A rigorous proof of heterogeneity can be obtained only by filtering the catalyst at the reaction temperature before completion of the reaction and then testing the filtrate for catalytic activity.[37] In order to check the stability of the TiO_2/HZSM-11(30%) catalyst, a 10^{-4} mol L^{-1} solution of 2CB containing 1 mg mL^{-1} of the photocatalyst was irradiated for 1 h. After that time TiO_2/HZSM-11(30%) was removed from the solution by filtration, and the remaining solution was irradiated for 3 more hours. The results obtained can be seen in Figure 7.

After the first hour, 2CB concentration decreased to 18% of its original value, keeping constant for 3 h thereafter. These results would indicate that TiO_2 does not become detached from the zeolite matrix, but remains attached throughout the reaction. In other words, there is then no detectable leaching of the catalyst in the reaction media. Consequently, TiO_2/HZSM-11(30%) catalyst is a very stable structure, which remains unchanged during whole reaction time.

Effect of H_2O_2 on the photocatalytic process

To investigate the effect of adding H_2O_2 on the photocatalysis of 2CB, experiments with four different amounts of H_2O_2 were carried out.

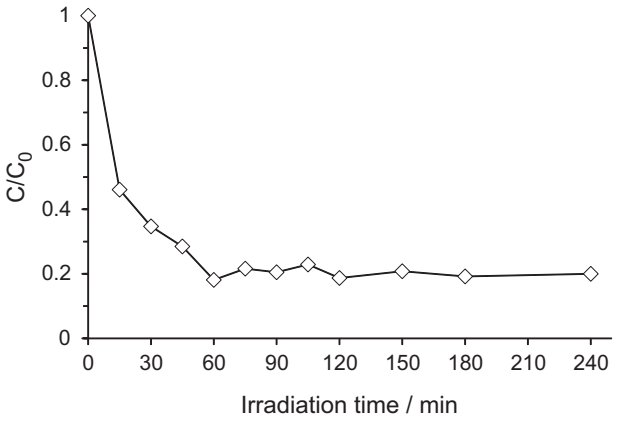

Figure 7. Leaching study: photocatalytic decomposition of 2CB over TiO_2/HZSM-11(30%).

The most important effect of adding H_2O_2 is the photogeneration of OH• radicals with UV light up to 350 nm,[38] as can be seen in equation 2. This should increase the reaction rate.

$$H_2O_2 \xrightarrow{h\upsilon} 2\ OH\bullet \quad (2)$$

However, other researchers[39] indicate that H_2O_2 can trap photo-induced electrons, and may partially contribute to the photodegradation rate with another mechanism (equation 3). This mechanism reduces the possibility of electron-holes recombination:

$$H_2O_2 \xrightarrow{e^-} OH^- + OH\bullet \quad (3)$$

In our research, OH• radicals cannot be generated as shown in equation 2 due to the wavelength range used (greater than 350 nm, see Experimental), but H_2O_2 could be reduced as seen in equation 3. For these reasons, the effect of H_2O_2 as electron acceptor was investigated (Figure 8).

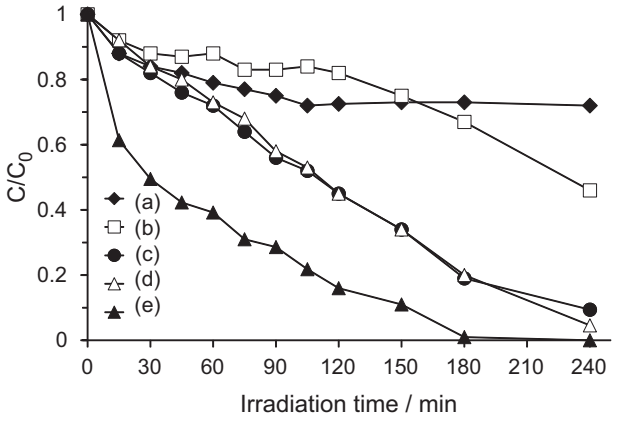

Figure 8. Photocatalytic decomposition of 2CB over TiO_2/HZSM-11(30%) with four different amounts of H_2O_2: (a) 2×10^{-3} mol L^{-1}, (b) 1×10^{-3} mol L^{-1}, (c) 5×10^{-4} mol L^{-1}, (d) 2.5×10^{-4} mol L^{-1}, and (e) without H_2O_2.

The experimental results show that none of the used amounts of H_2O_2 was effective to degrade 2CB in less than 3 h, as observed without the addition of H_2O_2. This result can be explained considering that the excess of H_2O_2 molecules can scavenge OH• radicals[40] generated either on the TiO_2 surface or by H_2O_2 as electron acceptor (equation 3).

At very low concentration (less than 2.5×10^{-4} mol L^{-1}), H_2O_2 should reach the TiO_2 surface before O_2 (concentration at saturation level: 2.6×10^{-4} mol L^{-1} at 25 ºC) without previous decomposition in H_2O and O_2, to compete with O_2 as electron acceptor. For this reason, H_2O_2 concentration less than 2.5×10^{-4} mol L^{-1} was not employed. With TiO_2, addition of H_2O_2 is valuable only if it can be used to generate OH• radicals with UV light, as can be seen in equation 2.

Influence of the relative position of Cl and COOH groups on an aromatic ring

Comparative photocatalytic degradation of 2CB, 3CB and 4CB

To assess the possible effect of the relative position of Cl and COOH on an aromatic ring, the photodegradation of 3CB and 4CB acids were carried out in the best conditions found for the photocatalysis of 2CB with TiO_2/HZSM-11(30%). The results obtained with 2CB, 3CB and 4CB compounds are shown in Figure 9.

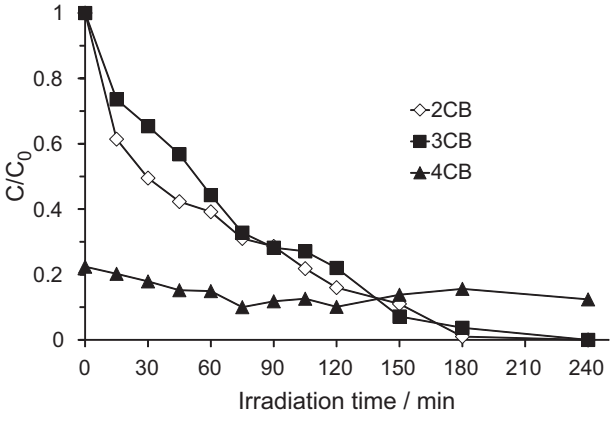

Figure 9. Photocatalysis of 2CB, 3CB and 4CB over TiO_2/HZSM-11(30%).

The degradation of 2CB and 3CB are similar, indicating that when Cl is in *ortho* or *meta* position with respect to the COOH group, the reactivity is comparable. It is also easy to see (Figure 9) that these compounds do not show significant adsorption on the zeolitic matrix during the equilibration time prior to irradiation.

However, 4CB shows a completely different behavior (Figure 9). During the equilibration time it is significantly adsorbed in the zeolitic matrix without further decomposition. The molecular diameter of 4CB may be similar to that of benzene (4.2 Å),[41] since both substituents are located on opposite ends of the molecule. If we consider that the pore size of zeolite is less than 5 or 6 Å by the partial obstruction with TiO_2 particles, 4CB could enter the interior of the zeolitic matrix, while 2CB and 3CB have a higher molecular diameter (6-7 Å), which does not facilitate their entry into the zeolitic matrix.

Adsorption of 2CB and adsorption and photocatalytic degradation of 4CB

Adsorption studies of 2CB and 4CB were carried out over HZSM-11 zeolite and TiO_2/HZSM-11(30%) catalyst at different concentration, as can be seen on Figure 10. 2CB is adsorbed in low proportion by TiO_2/HZSM-11(30%) catalyst and can be degraded under irradiation within 3 h, as can be seen on Figure 9.

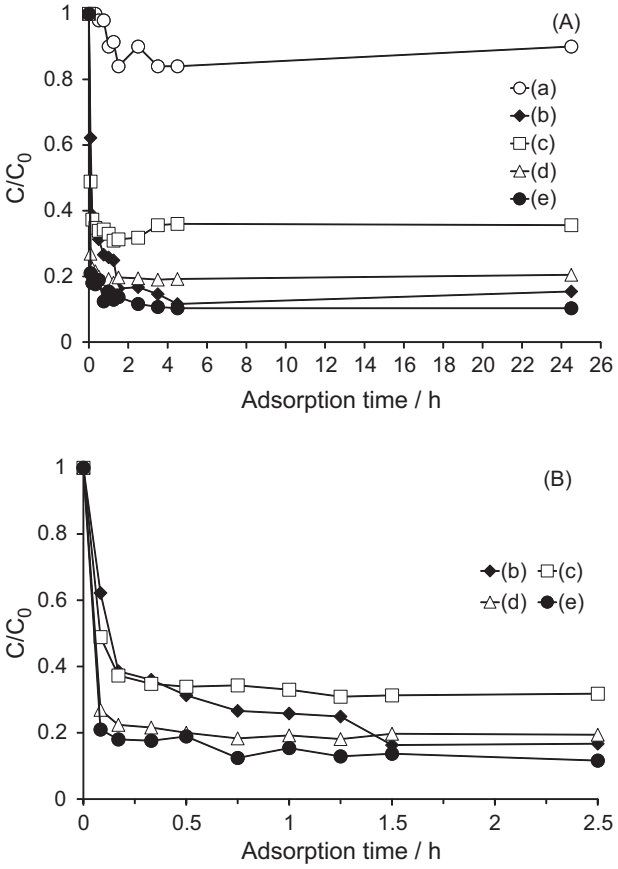

Figure 10. (A) Adsorption of 2CB over TiO_2/HZSM-11(30%) at (a) 1 mg mL^{-1}. Adsorption of 4CB over HZSM-11 (1 mg mL^{-1}, b) and TiO_2/HZSM-11(30%) at (c) 0.5 mg mL^{-1}, (d) 1 mg mL^{-1} and (e) 2 mg mL^{-1}. (B) Zoom of (A) between 0 and 2.5 h.

Adsorption of 4CB depends on catalyst concentration and is initially promoted by supported TiO_2. When the concentration of the photocatalyst increases the amount of adsorption sites increases as well, resulting in an

improvement of the adsorption rate. On the other hand, at pH value of 4CB solution (4.58) the TiO_2 surface is positively charged and a strong coulombic attraction between 4CB (pKa equal to 3.98) and the supported catalyst takes place. This fact would explain the different rates of adsorption of 4CB on the supported catalyst with respect to that observed for zeolite HZSM-11, within the first ninety minutes. 80 and 90% of initial 4CB concentration are retained by TiO_2/HZSM-11(30%) catalyst at 1 and 2 mg mL^{-1}, respectively, and 85% of this compound is strongly adsorbed by HZSM-11 zeolite after 24 h.

4CB is strongly adsorbed over TiO_2/HZSM-11(50%) catalyst (as noted above with TiO_2/HZSM-11(30%) catalyst) at the beginning of the photocatalysis process (Figure 11). This negatively-charged compound partially neutralizes the positively-charged TiO_2 surface. This fact weakens the driving force of the photocatalytic process, that is, the coulombic attraction between an ionizable compound and TiO_2 catalyst. Therefore, the amount of 4CB on solution decays slowly until the end of the irradiation time. However, a significant amount of 4CB remains strongly adsorbed on zeolitic matrix, ca. 80% of its original value (Figure 11). Sixty-two percent of the adsorbed compound may be released when the TiO_2/HZSM-11(50%) catalyst is suspended for 48 h in distilled water at pH 9. At this pH value, 4CB and TiO_2 are negatively charged; therefore this compound may be partially desorbed from the zeolite matrix by electrostatic repulsion.

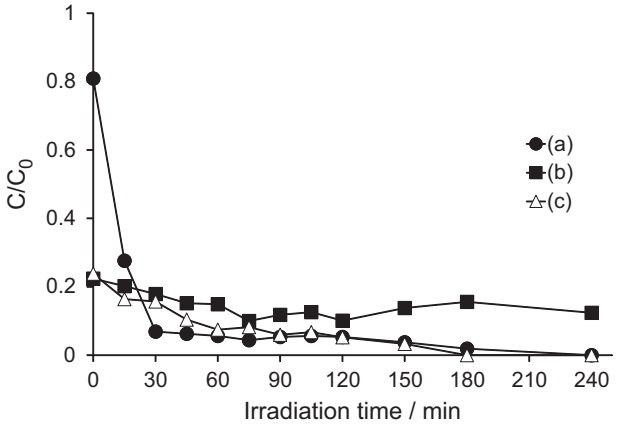

Figure 11. Photocatalysis of 4CB over (a) TiO_2 and (c) TiO_2/HZSM-11(50%) catalysts. For comparative purposes, photocatalysis of 4CB over (b) TiO_2/HZSM-11(30%) has been added to the figure.

Initially, unsupported TiO_2 was the most efficient catalyst to degrade 4CB. Nevertheless, after 45 min of irradiation there were no significant differences with respect to TiO_2/HZSM-11(50%) catalyst.

It is well known that the adsorption of many organic pollutants on different materials (e.g., activated carbon), on which TiO_2 is supported, significantly enhances their degradation, since it concentrates the substrate around the photocatalyst. However, if the substrate is strongly adsorbed, it cannot react with TiO_2 which precludes the decomposition.[42] This fact would explain the differences observed in the degradation of 2CB and 3CB with respect to 4CB. In other systems, the lack of adsorption of 4CB on the supporting material significantly influences its rate of decomposition. When TiO_2 is supported on glass fiber, 4CB adsorption on this material is null, and photodegradation occurs at a constant low rate.[43] However, TiO_2 immobilized on a ceramic surface is more efficient, degrading 64% of 4CB after 3 h of irradiation.[44] Moreover, HZSM-11 zeolite could be used to selectively adsorb the 4CB from polluted waterways, thus becoming an alternative method of environmental remediation.

Repeatability of the photocatalyst activity

The conservation of the catalytic activity of a photocatalyst is a very important factor, as it saves costs and materials, and simplifies removal and reuse. Photodegradation of 2CB with TiO_2/HZSM-11(30%) catalyst was carried out in several cycles in order to evaluate this property. Thus, a solution of 2CB with TiO_2/HZSM-11(30%) was irradiated for 3 h; then the catalyst was recovered by filtration and reused immediately, without any treatment, using a new solution of 2CB. Results obtained are shown in Figure 12.

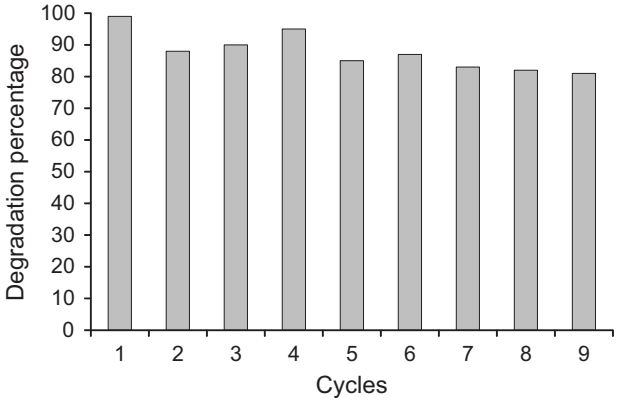

Figure 12. Activity study: photocatalysis of 2CB at different cycles. [2CB] = 10^{-4} mol L^{-1}; TiO_2/HZSM-11(30%) = 1 mg mL^{-1}.

As seen in Figure 12, the photocatalytic activity of TiO_2/HZSM-11(30%) is maintained above 80% degradation in all cases, with 88% average activity. This property of supported TiO_2 had already been proved successful on photodegradation of dyes,[7,45] toluene[46] and a β-cyclodextrin.[47] Our results show that the TiO_2/HZSM-11(30%) catalyst can

be reused immediately without previous reconditioning (e.g., catalyst drying), maintaining excellent photocatalytic activity for at least nine cycles.

Conclusions

We reported that TiO_2/HZSM-11(30%) catalyst, at a concentration of 1 mg mL^{-1}, was the most effective for completely degrading 2CB and 3CB after irradiation for 3 h. 4CB photodegradation was less effective with this catalyst. However, this compound can be partially degraded and/or removed from aqueous solutions by TiO_2/HZSM-11(50%) catalyst or HZSM-11 zeolite. Thus, the relative position of the substituents in the molecule is an important factor that influences the photodegradation rate of organic compounds with supported catalysts. Based on this, HZSM-11 zeolite could be used to selectively adsorb 4CB from polluted waterways, and therefore becomes an alternative method of environmental remediation.

According to our experiments, the TiO_2/HZSM-11(30%) catalyst is stable in solution, it retains its photocatalytic properties on 2CB after nine cycles, it can be easily removed from the treated solution and immediately reused. These are very important advantages of TiO_2/HZSM-11(30%) over unsupported TiO_2, making it a good photocatalyst for treatment of polluted waterways. Furthermore, this catalyst could be effective under solar irradiation, saving electrical energy.

Acknowledgements

This work was supported in part by MINCYT-Córdoba, UTN, CONICET, SECYT and ANPCyT. S. G. and J. P. M. gratefully acknowledge receipt of fellowships from CONICET. We wish to thank L. R. Pizzio for his cooperation.

References

1. He, Y.; Grieser, F.; Ashokkumar, M.; *J. Phys. Chem. A* **2011**, *115*, 6582.
2. Deavers, K.; Macek, T.; Karlson, U.; Trapp, S.; *Environ. Sci. Pollut. Res.* **2010**, *17*, 1355.
3. Li, X.; Zhang, Q.; Tang, L.; Lu, P.; Sun, F.; Li, L.; *J. Hazard. Mater.* **2009**, *163*, 115.
4. Zona, R.; Solar, S.; Getoff, N.; Sehested, K.; Holcman, J.; *Radiat. Phys. Chem.* **2010**, *79*, 626.
5. Muzikár, M.; Kresinová, Z.; Svobodová, K.; Filipová, A.; Cvancarová, M.; Cajthamlová, K.; Cajthaml, T.; *J. Hazard. Mater.* **2011**, *196*, 386.
6. Gandhi, V.; Mishra, M.; Rao, M.; Kumar, A.; Joshi, P.; Shah, D.; *J. Ind. Eng. Chem.* **2011**, *17*, 331.
7. Huang, M.; Xu, C.; Wu, Z.; Huang, Y.; Lin, J.; Wu, J.; *Dyes Pigm.* **2008**, *77*, 327.
8. Reddy, E.; Davydov, L.; Smirniotis, P.; *Appl. Catal., B* **2003**, *42*, 1.
9. Bhattacharyya, A.; Kawi, S.; Ray, M.; *Catal. Today* **2004**, *98*, 431.
10. Pan, Z.; Stemmler, E.; Cho, H.; Fan, W.; LeBlanc, L.; Patterson, H.; Amirbahman, A.; *J. Hazard. Mater.* **2014**, *279*, 17.
11. Mohamed, R.; Ismail, A.; Othman, I.; Ibrahim, I.; *J. Mol. Catal. A: Chem.* **2005**, *238*, 151.
12. Kanakaraju, D.; Kockler, J.; Motti, C.; Glass, B.; Oelgemöller, M.; *Appl. Catal., B* **2015**, *166-167*, 45.
13. Azzolina Jury, F.; Polaert, I.; Estel, L.; Pierella, L. B.; *Microporous Mesoporous Mater.* **2012**, *147*, 117.
14. Azzolina Jury, F.; Polaert, I.; Estel, L.; Pierella, L. B.; *Appl. Catal., A* **2013**, *453*, 92.
15. Gómez, S.; Leal Marchena, C.; Pizzio, L.; Pierella, L.; *J. Hazard. Mater.* **2013**, *258-259*, 19.
16. Renzini, M.; Sedrán, U.; Pierella, L. B.; *J. Anal. Appl. Pyrolysis* **2009**, *86*, 215.
17. Porkodi, K.; Arokiamary, S. D.; *Mater. Charact.* **2007**, *58*, 495.
18. Yamaguchi, S.; Fukura, T.; Imai, Y.; Yamaura, H.; Yahiro, H.; *Electrochim. Acta* **2009**, *55*, 7745.
19. Petkowicz, D.; Brambilla, R.; Radtke, C.; Silva da Silva, C.; da Rocha, Z. N.; Pergher, S. B.; dos Santos, J. H.; *Appl. Catal., A* **2009**, *357*, 125.
20. Anunziata, O. A.; Beltramone, A. R.; Juric, Z.; Pierella, L. B.; Requejo, F. G.; *Appl. Catal., A* **2004**, *264*, 93.
21. Kim, Y.; Yoon, M.; *J. Mol. Catal. A: Chem.* **2001**, *168*, 257.
22. Sing, K. S.; Everett, D. H.; Haul, R. A.; Moscou, L.; Pierotti, R. A.; Rouquerol, J.; Siemieniewska, T.; *Pure Appl. Chem.* **1985**, *57*, 603.
23. Zanjanchi, M. A.; Razavi, A.; *Spectrochim. Acta, Part A* **2001**, *57*, 119.
24. Petkowicz, D.; Pergher, S.; Silva da Silva, C.; da Rocha, Z.; dos Santos, J.; *Chem. Eng. J.* **2010**, *158*, 505.
25. Liqiang, J.; Xiaojun, S.; Weimin, C.; Zili, X.; Yaoguo, D.; Honggang, F.; *J. Phys. Chem. Solids* **2003**, *64*, 615.
26. Takeda, N.; Ohtani, M.; Torimoto, T.; Kuwabata, S.; Yoneyama, H.; *J. Phys. Chem.* **1997**, *101*, 2644.
27. Kavan, L.; Stoto, T.; Gratzel, M.; Fitzmaurice, D.; Shklover, V.; *J. Phys. Chem.* **1993**, *97*, 9493.
28. Li, Y.; White, T. J.; Lim, S. H.; *J. Solid State Chem.* **2004**, *177*, 1372.
29. Ohno, T.; Tagawa, S.; Itoh, H.; Suzuki, H.; Matsuda, T.; *Mater. Chem. Phys.* **2009**, *113*, 119.
30. Luís, A. M.; Neves, M. C.; Mendonça, M. H.; Monteiro, O. C.; *Mater. Chem. Phys.* **2011**, *125*, 20.
31. Ding, Z.; Hu, X.; Lu, G.; Yue, P.; Greenfield, P.; *Langmuir* **2000**, *16*, 6216.

32. Herrmann, J.; Guillard, C.; Disdier, J.; Lehaut, C.; Malato, S.; Blanco, J.; *Appl. Catal., B* **2002**, *35*, 281.
33. Ahmed, S.; Rasul, M.; Brown, R.; Hashib, M.; *J. Environ. Manage.* **2011**, *92*, 311.
34. Xiao, Q.; Zhang, J.; Xiao, C.; Si, Z.; Tan, X.; *Sol. Energy* **2008**, *82*, 706.
35. Colmenares, J. C.; Magdziarz, A.; *J. Mol. Catal. A: Chem.* **2013**, *366*, 156.
36. Li, G.; Lv, L.; Fan, H.; Ma, J.; Li, Y.; Wan, Y.; Zhao, X.; *J. Colloid Interface Sci.* **2010**, *348*, 342.
37. Pirkanniemi, K.; Sillanpaa, M.; *Chemosphere* **2002**, *48*, 1047.
38. Gupta, V.; Jain, R.; Agarwal, S.; Shrivastava, M.; *Colloids Surf., A* **2011**, *378*, 22.
39. Tseng, D.; Juang, L.; Huang, H.; *Int. J. Photoenergy* **2012**, DOI: 10.1155/2012/328526.
40. Castillo, N.; Ding, L.; Heel, A.; Graule, T.; Pulgarin, C.; *J. Photochem. Photobiol., A* **2010**, *216*, 221.
41. Krachenbuehl, F.; Stoeckli, F.; Addour, A.; Ehrburger, P.; Donnet, J.; *Carbon* **1986**, *24*, 483.
42. Shankar, M.; Cheralathan, K.; Arabindoo, B.; Palanichamy, M.; Murugesan, V.; *J. Mol. Catal. A: Chem.* **2004**, *223*, 195.
43. Enríquez, R.; Agrios, A.; Pichat, P.; *Catal. Today* **2007**, *120*, 196.
44. Dionysiou, D.; Suidan, M.; Baudin, I.; Laîné, J.; *Appl. Catal., B* **2004**, *50*, 259.
45. Yuan, R.; Zheng, J.; Guan, R.; Zhao, Y.; *Colloids Surf., A* **2005**, *254*, 131.
46. Lu, X.; Jiang, J.; Sun, K.; Cui, D.; *Appl. Surf. Sci.* **2011**, *258*, 1656.
47. Yuan, R.; Guan, R.; Zheng, J.; *Scr. Mater.* **2005**, *52*, 1329.

Submitted: October 21, 2014
Published online: April 7, 2015